JAERI-M
8451

放射性同位体製造資料－１２４３

SIMULATION OF THE ISOTOPIC RATIO DETERMINATION OF PLUTONIUM BY Ge(Li) γ-RAY SPECTROMETRY

September　１９７９

Hiroshi BABA, Hideyuki YAGI

日本原子力研究所
Japan Atomic Energy Research Institute

JAERI-M 8451

Simulation of the Isotopic Ratio Determination of Plutonium by Ge(Li) γ-Ray Spectrometry

Hiroshi BABA and Hideyuki YAGI[+]

Division of Radioisotope Production

Radioisotope Center, JAERI

(Received August 28, 1979)

A simulation prgram "SIMPUG" was developed for assessing feasibility of the isotopic ratio determination of plutonium by Ge(Li) γ-ray spectrometry. The program consists of (1) construction of the spectrum profiles for eight peak groupings of interest with a given set of isotopic compositions and by the use of the known nuclear data for emitting γ rays and (2) determination of the intensity of each participating nuclide following a presently developed algorithm of spectrum unfolding.

Effects of various factors on the reliability of the results were examined with the simulation program. Accuracy of the results was found to be little affected by the change of the detector resolution if the spectrum was taken with sufficient expansion. Counting statistics was concluded to be the most essential factor for the precision of the results, while the aging effect was not found significant. Contamination of fission products beyond a certain level brought about

---

+) Division of Reactor Engineering, Tokai Research Establishment

fatal errors in the determined values, particularly in the case of minor components.

Keywords: Simulation Program, Ge(Li) Detector, γ-Ray Spectrometry, Plutonium Isotopes, Isotopic Ratio, Nondestructive Analysis, Spectrum Unfolding, Accuracy

JAERI—M 8451

Ge(Li) γ線スペクトロメトリによるプルトニウム同位体比決定法のシミュレーション

日本原子力研究所アイソトープ事業部製造部
馬場　宏・八木秀之+

（1979年8月28日受理）

Ge (Li) γ線スペクトロメトリによるプルトニウム同位体比の決定法の有用性を調べる目的で，シミュレーションプログラムSIMPUGを開発した。このプログラムは次の2つの部分から成っている。第1部では，プルトニウムのγ線スペクトル中で特に重要な8つのピーク群のそれぞれについて，γ線核データを既知のものとして，与えられた同位体存在比の試料の与えるスペクトルを合成する。次に第2部では，既に開発済みの同位体比決定法に従って，逆にこの合成スペクトルを解析して各寄与核種の存在比を求め，最初に入力した相対存在量と比較する。

このシミュレーションプログラムを用いて，解析精度に対する種々の因子の影響を調べた。最初に，検出器の分解能の影響を調べたが，この因子はスペクトルが充分なチャネル数に広げて測定されているならば結果の信頼性に殆んど影響しないことが見出された。結果の精度に最も大きな影響を及ぼす因子は計数の統計精度であった。反面危惧されていた試料の経年効果はあまり問題にならないことが結論された。最後に，核分裂生成核種（FP）が混在する場合の影響を調べた結果，FPの存在量がある限界量を越すと急激に信頼性が低下することが見出され，この傾向は微少成分において特に顕著であった。

+）東海研究所原子炉工学部

Contents

1. Introduction 1
2. Bases of the Simulation Program 3
3. Simulation Program SIMPUG 5
4. Results and Discussion 8
5. Conclusion 14
References 15
Tables 16
Figures 24

目　　次

1. 序　論 …… 1
2. シミュレーション・プログラムの基本方針 …… 3
3. シミュレーション・プログラムSIMPUG …… 5
4. 結果と考察 …… 8
5. 結　論 …… 14
文　献 …… 15
表 …… 16
図 …… 24

1. Introduction

In the complete analysis of plutonium, high-resolution γ-ray spectrometry is proposed for determination of the isotopic ratios[1-3]. Non-destructive γ-ray spectrometry has obvious advantage in a sense of the manageability of a large number of samples over more reliable but tedious destructive methods. It is particularly the case for the field measurement of plutonium samples.

One of the main disadvantages of the non-destructive analysis of solid samples was the uncertainty in the counting efficiency of γ-ray attenuation by the sample matrix or other absorbing materials. Now, the difficulty has been successfully removed by the spectrum unfolding technique with narrow peak groupings[4,5]. Gunnink has developed a simulation program to set up appropriate peak groupings for determination of the ratios among plutonium isotopes and ^{241}Am, one of the daughter nuclides, and worked out the feasibility test of the analyzing method by applying it to samples of various isotopic grades[4]. He has shown that the isotopic ratios are very well reproduced for the case of fresh and clean plutonium samples, i.e. those of low americium content and without contamination of the fission product nuclides.

In the real occasions, however, one must face rather dirty samples containing considerable amounts of fission products and ^{241}Am, as we did experience elsewhere[5]. In the previous work[5], we have developed a computerized analyzing method "PASAY" in which we have utilized peak groupings some-

what different from those taken by Gunnink. He has selected peak multiplets in low energy region, while our groupings locate higher energy region as shown in Fig.1. This is the consequence of our experimental condition[5] in which low-energy γ rays and X rays were strongly attenuated for suppressing strong radiations from ^{241}Am (cf. Fig.15 of ref.5).

Therefore, one needs to investigate the feasibility of the analyzing method developed for realistic sample measurements under much severe counting condition. Much effort would be required in order to assess the effects of various factors on the precision through experimental studies on one hand, and through certain means making up the deficiency of experiments. The latter would particularly be important because it is not easy to preparing varieties of the testing material.

A simulation program "SIMPUG" was then developed to carry out the feasibility test of the algorithm of "PASAY" with far more easiness and the effect of various factors on the reliability of the result was discussed.

2. Bases of the Simulation Program

As is shown in Table 1, eight peak groupings were chosen as the key multiplets for determining the isotopic ratios. Thses key multiplets are coloured in red in Fig.1, while the other groupings depicted in black colour play subsidiary roles and therefore not included in the present simulation. For example, the groups I and II may supply reliable information for samples of low americium content. However, it is not always the case because of the sharp change in the efficiency and γ attenuation in this energy range as shown in ref.5.

Gunnink has performed the simulation study for five different isotopic blends based on a classification scheme given by Bishop and Taylor[6]. However, we have utilized two blends for which we know the contents of not only plutonium isotopes but also the decay products such as ^{241}Am, ^{228}Th, and typical fission product nuclides.

The spectrum profile of a given grouping can be constructed on the basis of known energies and intensities of all the γ rays involved for a given set of isotopic ratios and counting condition concerning the peak width, peak asymmetry, and statistics. There is, however, one factor indispensable to construct a nearly real spectrum. That is, the functional form of the underground background continuum.

As discussed elsewhere[7], it has been shown that supperposition of the step functions is sufficiently good as the background shape, which is straightforwardly built if the heights of both boundaries of the grouping are given. We

have deduced the relationship roughly representing the heights of the boundaries as the function of the contents of the isotopes including fission products from the works undertaken in ref.5. The resulting relationships are summarized in Table 2.

3. Simulation Program SIMPUG

The program is divided into two parts. The first part involves the synthesis of the simulation spectrum for each of the selected eight peak groupings (cf. Table 1) under a particular set of conditions. Here, the parameters whose values are to be given are the peak width, peak asymmetry[8], energy-to-channel conversion ratio, total counts of the γ rays emitted from each isotope, initial number to be given to a pseudorandom series of the Poisson distribution, the number of the repeated runs. Half lives and the energies and branching ratios[9,10] of the concerned γ rays are stored in the program for relevant eight nuclides; namely, $^{238\text{-}241}$Pu, ^{241}Am, ^{228}Th, ^{95}Zr-^{95}Nb, and ^{144}Ce.

The synthesized spectrum is of the form:

$$\underline{Y}(\underline{x}) = \sum_{i=1}^{n} \underline{y}_i(\underline{x}) + \underline{B}(\underline{x}), \tag{1}$$

where $\underline{Y}(\underline{x})$ is the resulting total counts at channel $\underline{x}$ which is the sum of the spectrum profiles of all the involved nuclides, $\underline{y}(\underline{x})$, and the background continuum, $\underline{B}(\underline{x})$. The spectrum profile $\underline{y}_i$ is in turn constructed with known γ-ray data as

$$\underline{y}_i(\underline{x}) = \underline{P}\cdot\underline{A}_i \sum_{j=1}^{m} \phi_j \underline{f}_j(\underline{x};\underline{x}_0,\sigma,\omega), \tag{2}$$

where $\underline{P}$ is the Poisson random number, $\underline{A}_i$ the intensity of the $\underline{i}$th nuclide, ϕ_j the branching ratio of the $\underline{j}$th γ ray of the relevant nuclide, and

$$\underline{f}_j(\underline{x};\underline{x}_0^j,\sigma,\omega) = \begin{cases} \exp\{-(\underline{x}-\underline{x}_0^j)^2/\sigma\} & \text{for } \underline{x} < \underline{x}_0^j \\ \exp\{-(\underline{x}-\underline{x}_0^j)^2/\omega\sigma\} & \text{for } \underline{x} > \underline{x}_0^j \end{cases} \tag{3}$$

with the peak channel $\underline{x}_0^j$, width parameter σ, and asymmetry factor ω.

The background function $\underline{B}(\underline{x})$ is given by

$$\underline{B}(\underline{x}) = \underline{P}(\underline{h}_2-\underline{h}_1) \sum_{j=1}^{k} \underline{p}_j \underline{S}(\underline{x}-\underline{x}_0^j) \Big/ \sum_{i=1}^{k} \underline{p}_i + \underline{h}_1 \ , \qquad (4)$$

where $\underline{h}_1$ and $\underline{h}_2$ are the counts at the boundaries of the grouping in the low- and high-energy sides, and $\underline{p}_j$ is the height of the $\underline{j}$th peak among $\underline{k}$ prominent peaks in the grouping. $\underline{S}$ is a step function defined by

$$\underline{S}(\underline{x}) = \begin{cases} 0 & \text{for } \underline{x} < 0 \\ 0.5 & \text{for } \underline{x} = 0 \\ 1 & \text{for } \underline{x} > 0 \end{cases} \qquad (5)$$

In the second part of the program, unfolding of the spectrum synthesized in the first part is carried out by the linear least squares method based on the normalized composite response profiles of all the participating nuclides. In the unfolding procedure, one can chose either of the options of fixing the peak positions and width at the initially given values or varying them as free parameters. Readjustment of the parameters is performed by the non-linear function minimizing method[11]. As for the peak positions, they are parallelly shifted in the fitting process since the error in the channel-to-energy conversion ratio would introduce practically no significant difference in the mutual separations within such a narrow range.

The main purpose of the present simulation was of course to study the accuracy of the isotopic ratios under the influence of various factors, such as isotopic grade, counting

statistics or contamination of the fission products. There was, however, another purpose of as much importance to figure out the way of evaluating the associating error correctly. This is important because we need to know reliable allowance interval for the predicted values deduced from rather rough data in the field work.

Generally speaking, the error associated with the deduced content of a given nuclide consists of the following two components. The first component is an error due to the uncertainty in the background continuum and the second one is the error associated with the unfolding process itself. Moreover, the latter is affected by the statistical fluctuations and the inaccuracies in the determined contents of the remaining nuclides.

4. Results and Discussion

Two sets of the isotopic composition were studied in the present work and they are summarized in Table 3. The conversion gain was fixed to 0.25 keV/channel and the symmetric peak shape was assumed throughout the studies.

The effect of the peak width on the precision was first examined for the full width at half maximum (FWHM) from 1.0 to 2.25 keV. It turned out that the reliability was little affected by the change in the peak width. Therefore, the FWHM was fixed to the value given by the following equation:

$$\mathrm{FWHM} = 1.125 + 6.25\times10^{-4}\underline{E}\ (\mathrm{keV}), \qquad (6)$$

which was nearly equal to the resolution of one of the Ge(Li) detectors used in the field experiment[5].

The next study was carried out for investigating how the predicted values converged within the allowance interval given by the errors evaluated as the statistical fluctuation being varied. The resulting contents of five main isotopes relative to the content of ^{239}Pu are displayed through Figs.2 to 6. Here, the variable on the abscissa is the number of counts which one would obtain with the ficticious γ ray of ^{239}Pu having the branching ratio of 1×10^{-6}. Simulation was repeated three times for each simulation condition.

As one sees in Figs.2 and 3, the relative abundance of ^{241}Pu can be obtained with group IV and V, while that of ^{241}Am is determinable with groups, IV, V, and VI. The figures clearly indicate that they were best determined with group IV; the attached error was always the smallest and the deviation

from the true value stayed within the error all the time.

The relative abundance of ^{240}Pu is important from the following reason that the isotopic grade of ^{239}Pu sample is mostly depending on the above quantity because it is more than one order of magnitude greater compared to the contents of the remaining plutonium isotopes. Therefore, the fissile-to-total plutonium ratio is also affected by the precision of the ^{240}Pu content. Grouping IX and XI were utilized for determining the quantity. Here, the relative content, $^{241}Am/^{239}Pu$, was fixed to the value obtained with group IV.

The results in Figs.4 indicate that one can not expect reliable results with group XI and should rely on those found with group IX. One can conclude from Figs.4 that the statistics of $2\text{-}5\times10^{3}$ counts or more is required in order to assure 1% precision in the isotopic grade of ^{239}Pu.

The content of ^{238}Pu can be deduced in the unfolding of the groupings XIII and XIV. The $^{241}Am/^{239}Pu$ ratio was again fixed to the previously determined value. It can be concluded that both groupings can give nearly equally good results and the estimated errors were of reasonable order of magnitude. It should, however, be mentioned that the resul with group XIV eventually becomes very poor due to mis-estimation of the background continuum in the case of low ^{238}Pu content and poor statistics.

There appear γ rays from ^{228}Th as the daughter of ^{236}Pu and/or ^{232}U in the spectrum. The content of ^{228}Th is therefore worth to know as an information on those precursors.

The content of ^{228}Th was deduced from the groupings XII and XIII with fixing $^{241}Am/^{239}Pu$ as before. Figures 6 show that the result with group XIII is less reliable and the lower limit for determination of $^{228}Th/^{239}Pu$ would be about 5×10^{-10}.

Plutonium-241 decays to ^{241}Am with the half life of 15y. The content of the latter increases as the storage duration increases. This means that one must expect more interference of ^{241}Am against precise determination of the isotopic grade of aged plutonium samples.

We then attempted a simulation test for the consequence of the sample analysis with various ^{241}Am contents. In the test, the isotopic abundances were assumed to be those of the 75% sample given in Table 3, except for those of ^{241}Pu and ^{241}Am. Instead, the sum of them was taken to be constant. The variable on the abscissa through Figs.7 to 9 is the ratio between $^{241}Am/^{239}Pu$ and $^{241}Pu/^{239}Pu$. Furthermore, good statistical condition, the case of 2×10^{4} counts (cf. Fig.2b), was chosen so that we could see the aging effect only without being interfered by the statistical effect.

Figures 7 to 9 clearly indicate that the aging effect does not affect much the precision of the determination of the isotopic abundances even for rather dirty ^{239}Pu sample. For $^{238}Pu/^{239}Pu$, the groupings XIII and XIV both assured equally good precision, while the groupings IX and XII gave much more reliable results for $^{240}Pu/^{239}Pu$ and $^{228}Th/^{239}Pu$, respectively, than the alternatives did.

The last investigation was about the effect of fission-

product (FP) contamination on the reliability of the unfolding results. This effect is two-fold; firstly, they raise the background continuum in every peak grouping as shown in Table 2, and secondly, the appearance of the spectrum is changed in some groupings. For example, the 724-keV photopeak of ^{95}Zr becomes prominent in the group XII, while the ^{95}Zr 757-keV and ^{95}Nb 766-keV peak appear in the grouping XIII. Furthermore, the 696-keV peak from ^{144}Ce is observed in the grouping XI.

In the succeeding test, the isotopic abundances were fixed to the value listed in Table 3 except for the contents of the fission products. The relative abundances of fission product nuclides were then varied by several orders of magnitude with keeping the ratios among themselves constant. Here, the statistics of ^{239}Pu γ rays was fixed to 1×10^{3} for the 92% and to 2×10^{3} counts for the 75% sample, respectively. These values of statistics were nearly the same as the case of the field experiment[5].

The results of the test are presented through Figs.10 to 14, where the isotopic abundance of ^{95}Zr relative to that of ^{239}Pu is taken as the abscissa. In the determination of ^{241}Pu/^{239}Pu, the grouping V is not much dependable particularly in the case of high-grade ^{239}Pu samples. The reliability of the group IV is lost when the content of ^{95}Zr exceeds about 5×10^{-10}, as seen in Figs.10. One can expect equally high precision for ^{241}Am/^{239}Pu determined with the group IV as indicated in Figs.11.

The unfolding results on $^{240}Pu/^{239}Pu$ show somewhat different tendency from that of the above cases. In the case of the 92% sample, the result with group IX is far more reliable than that of group XI for low FP contents. However, the former rapidly loses its reliability as the FP content increases while the latter is little affected by increasing FP content (cf. Fig.12a). Consequently, the latter becomes even more reliable than the former at high FP contents.

The situation is much different with the low grade sample. The superiority of the grouping IX over XI is kept for the ^{95}Zr content as high as 5×10^{-10}, and the resulting $^{240}Pu/^{239}Pu$ ratio is fairly good even at the FP content ten times greater (cf. Fig.12b).

Accurate determination of the ^{238}Pu content is rather difficult because it is a minor component. Judging from the results given in Figs.13, the lower limit of the content that guarantees more or less reliable result seems to be a few tenths per cent. The grouping XIII gave better result for low FP contents, whereas the result with group XIV became better when the FP content was high.

Now that we are sure for accurate determination of the $^{95}Zr/^{239}Pu$ with grouping XII, it is worthy of investigating the feasibility of a modification of determination of the ^{238}Pu content with group XIII. That is, one fix the $^{95}Zr/^{239}Pu$ ratio as well as the $^{241}Am/^{239}Pu$, and try to deduce the $^{238}Pu/^{239}Pu$ ratio by unfolding the grouping XIII.

There seems to be a limit below which one can not expect

reliable results on the $^{228}Th/^{239}Pu$ value. The limit was found to lie around $5x10^{-10}$, as one would conclude from Figs.14.

5. Conclusion

The present simulation work "SIMPUG" based on the analyzing program "PASAY" showed that the algorithm of the program would assure sufficient precision for the isotopic ratio determination of plutonium samples, if the counting statistics is not very poor. The resulting precision was little affected by the increase of the ^{241}Am content within a practicable range. This means that aged samples can be analyzed with as much reliability as fresh ones.

The effect of the short-lived fission product (FP) contamination on the accuracy was observed for large values of the FP content. As a result of simultion, there existed certain critical value in the FP content above which obtained isotopic ratios became unreliable. This critical content was about 10^{-10} as the atomic ratio between ^{95}Zr and ^{239}Pu within the framework of the present simulation.

The error introduced in the determination of the isotopic ratios was found depending mostly on the statistical fluctuation. It was possible to obtain very accurate consequences by improving the statistics for samples whose FP contents were not very high. It follows that measuring the spectrum with as good statistics as possible is the most important of all. One should therefore keep in mind that acquisition of one spectrum data needs to be continued for 4-5 hours at the total count rate of maximum 5,000 cps (if pile-up rejector is not used), or triplicate or more measurements of 1 hour duration are required.

References

1. R.Gunnink, J.B.Niday, and P.D.Siemens, UCRL-51577 Pt.1 (1974).
2. T.N.Dragnev, J. Radioanal. Chem. 36 (1977) 491.
3. R.Gunnink, UCRL-80464 (1978).
4. R.Gunnink, UCRL-51605 (1974).
5. H.Baba, T.Suzuki, Y.Nakahara, H.Yagi, and S.Okazaki, JAERI-M 8450 (1979).
6. D.M.Bishop and I.N.Taylor, General Electric Co. Report NEDO-12467 (1973).
7. H.Baba, S.Baba, and T.Suzuki, Nucl. Instr. and Methods 145 (1977) 517.
8. H.Baba, T.Sekine, S.Baba, and H.Okashita, JAERI 1227 (1973).
9. R.Gunnink, J.E.Evans, and A.L.Prindle, UCRL-52139 (1976).
10. W.W.Bowman and K.W.MacMurdo, Atomic Data and Nuclear Data Tables, Vol.13, Nos.2-3 (1974).
11. T.Shimanouchi and I.Suzuki, J. Chem. Phys. 42 (1965) 296.

Table 1. Eight important peak groupings used for isotopic ratio determination. Tabulations specify energy range of each grouping, sources, energies and intensities of γ rays, and references. minor γ components are occasionally neglected.

Source	Energy(keV)	Intensity	Reference
Group IV (329.5 - 346.5 keV)			
^{241}Pu-^{237}U	332.354	2.98×10^{-7}	9
^{241}Am	332.354	1.49×10^{-6}	9
^{239}Pu	332.838	5.06×10^{-6}	9
^{241}Pu-^{237}U	335.405	2.39×10^{-8}	9
^{241}Am	335.405	4.96×10^{-6}	9
^{239}Pu	336.107	1.134×10^{-6}	9
^{241}Am	337.72	4.29×10^{-8}	9
^{239}Pu	341.510	6.62×10^{-7}	9
^{239}Pu	345.014	5.59×10^{-6}	9
Group V (366.0 - 384.5 keV)			
^{239}Pu	367.050	8.65×10^{-7}	9
^{239}Pu	368.550	9.03×10^{-7}	9
^{241}Pu-^{237}U	368.605	1.05×10^{-8}	9
^{241}Am	368.605	2.17×10^{-6}	9
^{241}Pu-^{237}U	370.934	2.71×10^{-8}	9
^{241}Am	370.934	5.23×10^{-7}	9
^{239}Pu	375.042	1.57×10^{-5}	9
^{241}Am	376.595	1.38×10^{-6}	9
^{239}Pu	380.166	3.05×10^{-6}	9
^{239}Pu	382.751	2.59×10^{-6}	9
^{241}Am	383.74	2.82×10^{-7}	9
Group VI (409.0 - 431.0 keV)			
^{239}Pu	411.15	6.8×10^{-8}	9
^{239}Pu	413.712	1.489×10^{-5}	9
^{241}Am	419.24	2.87×10^{-7}	9
^{239}Pu	422.586	1.193×10^{-6}	9
^{241}Am	426.39	2.46×10^{-7}	9
^{239}Pu	426.68	2.328×10^{-7}	9
^{239}Pu	428.4	1.00×10^{-8}	9
^{241}Am	429.84	1.15×10^{-8}	9
^{239}Pu	430.08	4.30×10^{-8}	9
Group IX (630.0 - 649.0 keV)			
^{241}Am	633.0	1.26×10^{-8}	9
^{239}Pu	633.15	2.53×10^{-8}	9

Table 1. (continued)

Source	Energy (keV)	Intensity	Reference
^{239}Pu	637.837	2.56×10^{-8}	9
^{239}Pu	640.075	8.20×10^{-8}	9
^{241}Am	641.42	7.10×10^{-8}	9
^{240}Pu	642.48	1.245×10^{-7}	9
^{239}Pu	645.969	1.489×10^{-7}	9
	Group XI (684.0 - 711.5 keV)		
^{240}Pu	687.7	3.55×10^{-8}	9
^{241}Am	688.77	3.25×10^{-7}	9
^{241}Am	693.49	3.68×10^{-8}	9
^{144}Ce	696.4	1.5×10^{-2}	10
^{241}Am	696.44	5.34×10^{-8}	9
^{239}Pu	701.1	5.12×10^{-9}	9
^{239}Pu	703.73	3.95×10^{-8}	9
^{241}Am	709.41	6.41×10^{-8}	9
	Group XII (716.0 - 732.0 keV)		
^{239}Pu	717.72	2.74×10^{-8}	9
^{239}Pu	720.3	4.85×10^{-10}	9
^{241}Am	721.990	1.96×10^{-6}	9
^{95}Zr	724.18	4.3×10^{-1}	10
^{228}Th	727.28	6.36×10^{-2}	10
^{239}Pu	727.9	1.24×10^{-9}	9
^{241}Am	729.52	1.33×10^{-8}	9
	Group XIII (753.5 - 773.5 keV)		
^{241}Am	755.91	7.60×10^{-8}	9
^{239}Pu	756.40	3.47×10^{-8}	9
^{95}Zr	756.72	5.46×10^{-1}	10
^{241}Am	759.46	1.67×10^{-8}	9
^{228}Th	763.34	5.78×10^{-3}	10
^{241}Am	763.4	1.96×10^{-9}	9
^{239}Pu	763.7	3.24×10^{-10}	9
^{95}Zr-^{95}Nb	765.79	9.9×10^{-1}	10
^{238}Pu	766.41	2.19×10^{-7}	9
^{239}Pu	766.6	2.75×10^{-9}	9
^{241}Am	766.92	5.00×10^{-8}	9
^{239}Pu	769.37	1.12×10^{-7}	9
^{241}Am	770.58	4.74×10^{-8}	9
^{241}Am	772.13	2.66×10^{-8}	9

Table 1. (continued)

Source	Energy (keV)	Intensity	Reference	Source	Energy (keV)	Intensity	Reference
	Group XIV (735.0 - 745.0 keV)						
^{241}Am	737.29	8.00×10^{-8}	9				
^{238}Pu	742.82	5.17×10^{-8}	9				

Table 2. Heights of the background level at the boundaries of each peak grouping.

Grouping	$\underline{h}_1$	$\underline{h}_2$
IV	$0.11[P9]_{333} + 0.03[P1]_{332} + 0.2\underline{N}_{Nb}\times10^{13}$	$0.89\underline{h}_1$
V	$0.34[P9]_{369} + 0.14[Al]_{369} + 0.8\underline{N}_{Nb}\times10^{13}$	$0.55\underline{h}_1$
VI	$0.011[P9]_{414} + 0.8[Al]_{419} + 0.2\underline{N}_{Nb}\times10^{13}$	$0.4\underline{h}_1$
IX	$0.15[P9]_{649} + 0.15[Al]_{653} + 0.07\underline{N}_{Nb}\times10^{13}$	$\underline{h}_1$
XI	$0.2[P9]_{704} + 0.1[Al]_{689} + 0.04\underline{N}_{Nb}\times10^{13}$	$\underline{h}_1$
XII	$0.3[P9]_{718} + 0.015[Al]_{722} + 0.03\underline{N}_{Nb}\times10^{13}$	$0.8\underline{h}_1$
XIII	$0.22[P9]_{756} + 0.20[Al]_{756} + 0.04\underline{N}_{Nb}\times10^{13}$	$0.75\underline{h}_1$
XIV	$0.32[Al]_{737} + 0.05\underline{N}_{Nb}\times10^{13}$	$\underline{h}_1$

$[P9]_E$: peak height of the $\underline{E}$-keV ^{239}Pu γ ray

$[P1]_E$: peak height of the $\underline{E}$-keV ^{241}Pu γ ray

$[Al]_E$: peak height of the $\underline{E}$-keV ^{241}Am γ ray

$\underline{N}_{Nb}$: the number of atoms of ^{95}Nb relative to that of ^{239}Pu

Table 3. Two sets of the isotopic ratios assumed in the present simulation work.

Nuclide	92% sample	75% sample
^{238}Pu	8.0×10^{-4}	3.5×10^{-3}
^{239}Pu	1.0	1.0
^{240}Pu	1.0×10^{-1}	1.6×10^{-1}
^{241}Pu	7.0×10^{-3}	3.5×10^{-2}
^{241}Am	4.0×10^{-3}	1.75×10^{-2}
^{228}Th	3.0×10^{-11}	2.0×10^{-10}
^{95}Zr-^{95}Nb	7.0×10^{-12}	5.0×10^{-13}
^{144}Ce	5.0×10^{-12}	1.5×10^{-12}

Figure Captions

Fig.1. Gamma-ray spectrum of a plutonium sample, the counting condition for which is described elsewhere[5]. Roman numerals specify the peak groupings to be used in the analysis. Peak groupings marked with red colour are the key multiplets for the isotopic ratio determination, and are studied in the present simulation.

Fig.2. Relative abundance of ^{241}Pu to ^{239}Pu versus statistical condition. Two peak groupings, IV and V, were the subject of study and triplicate runs were carried out in order to investigate the statistical fluctuation. A horizontal line in the middle indicates the pre-set (assumed) value. The variable in the abscissa gives the strength of the ^{239}Pu spectrum profile (see text).

Fig.3. Relative abundance of ^{241}Am to ^{239}Pu versus statistical condition. Three peak groupings, IV, V, and VI, were the subject of study. For further details, see the caption of Fig.2.

Fig.4. Relative abundance of ^{240}Pu to ^{239}Pu versus statistical condition. Two peak groupings, IX and XI, were the subject of study. For further details, see the caption of Fig.2.

Fig.5. Relative abundance of ^{238}Pu to ^{239}Pu versus statistical condition. Two peak groupings, XIII and XIV, were the subject of study. For further details, see the caption of Fig.2.

Fig.6. Relative abundance of ^{228}Th to ^{239}Pu versus statistical condition. Two peak groupings, XII and XIII, were the subject of study. For further details, see the caption of Fig.2.

Fig.7. Aging effect on the precision of the relative abundance of ^{240}Pu for the case of the 75% ^{239}Pu sample. The variable of the abscissa is the ratio between $^{241}Am/^{239}Pu$ and $^{241}Pu/^{239}Pu$.

Fig.8. Aging effect on the precision of the relative abundance of ^{238}Pu for the case of the 75% ^{239}Pu sample. The variable of the abscissa is the ratio between $^{241}Am/^{239}Pu$ and $^{241}Pu/^{239}Pu$.

Fig.9. Aging effect on the precision of the relative abundance of ^{228}Th for the case of the 75% ^{239}Pu sample. The variable of the abscissa is the ratio between $^{241}Am/^{239}Pu$ and $^{241}Pu/^{239}Pu$.

Fig.10. Effect of the FP contamination on the precision of the relative abundance of ^{241}Pu. The variable of the

abscissa is the relative abundance of ^{95}Zr to ^{239}Pu.

Fig.11. Effect of the FP contamination on the precision of the relative abundance of ^{241}Am. The variable of the abscissa is the relative abundance of ^{95}Zr to ^{239}Pu.

Fig.12. Effect of the FP contamination on the precision of the relative abundance of ^{240}Pu. The variable of the abscissa is the relative abundance of ^{95}Zr to ^{239}Pu.

Fig.13. Effect of the FP contamination on the precision of the relative abundance of ^{238}Pu. The variable of the abscissa is the relative abundance of ^{95}Zr to ^{239}Pu.

Fig.14. Effect of the FP contamination on the precision of the relative abundance of ^{228}Th. The variable of the abscissa is the relative abundance of ^{95}Zr to ^{239}Pu.

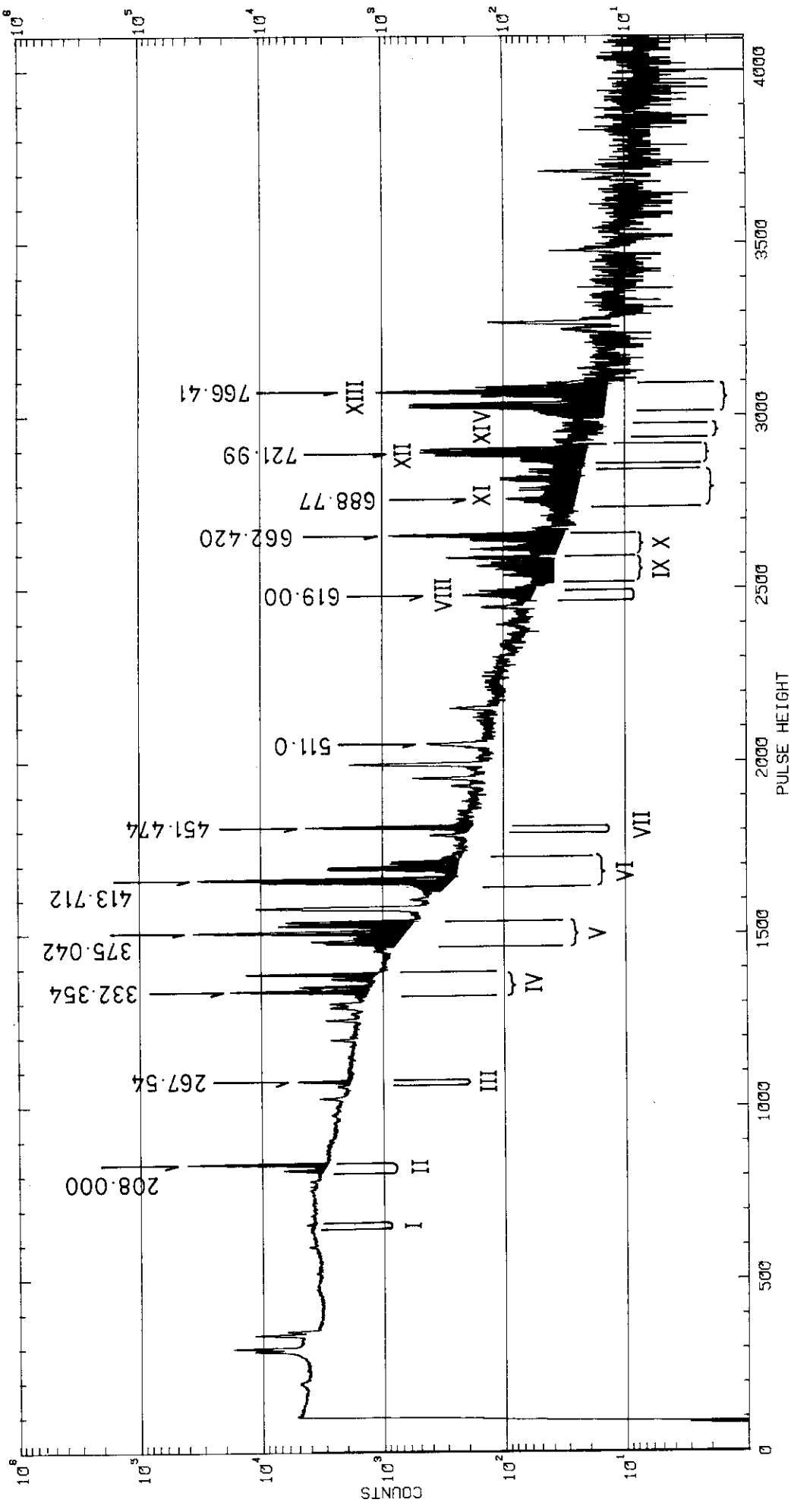
COUNTS
PULSE HEIGHT
208.000
267.54
332.354
375.042
413.712
451.474
511.0
619.00
662.420
688.77
721.99
766.41
I
II
III
IV
V
VI
VII
VIII
IX
X
XI
XII
XIII
XIV

Fig.1

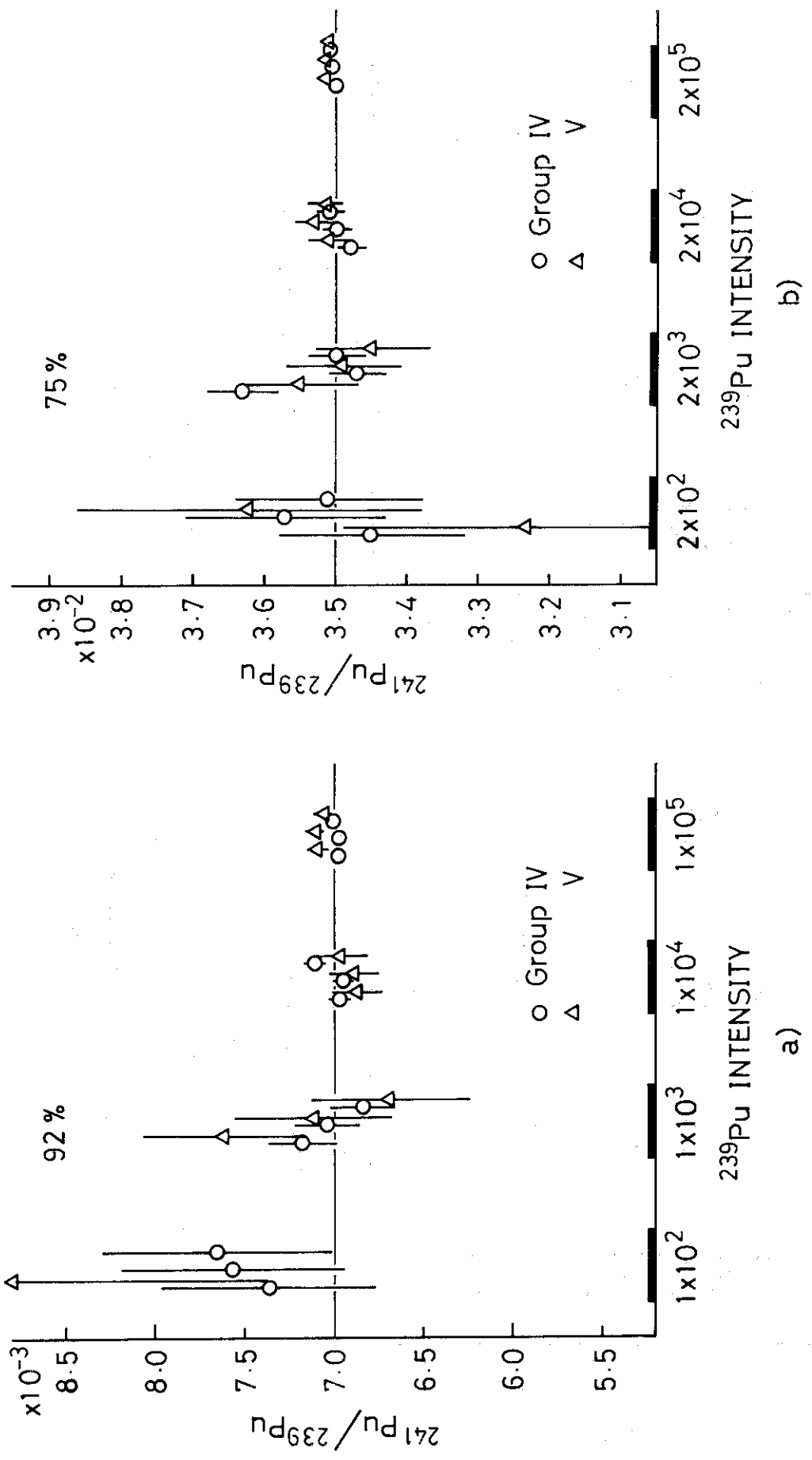

Fig.2. Relative abundance of ^{241}Pu to ^{239}Pu versus statistical condition. Two peak groupings, IV and V, were the subject of study and triplicate runs were carried out in order to investigate the statistical fluctuation. A horizontal line in the middle indicates the pre-set (assumed) value. The variable in the abscissa gives the strength of the ^{239}Pu spectrum profile (see text).

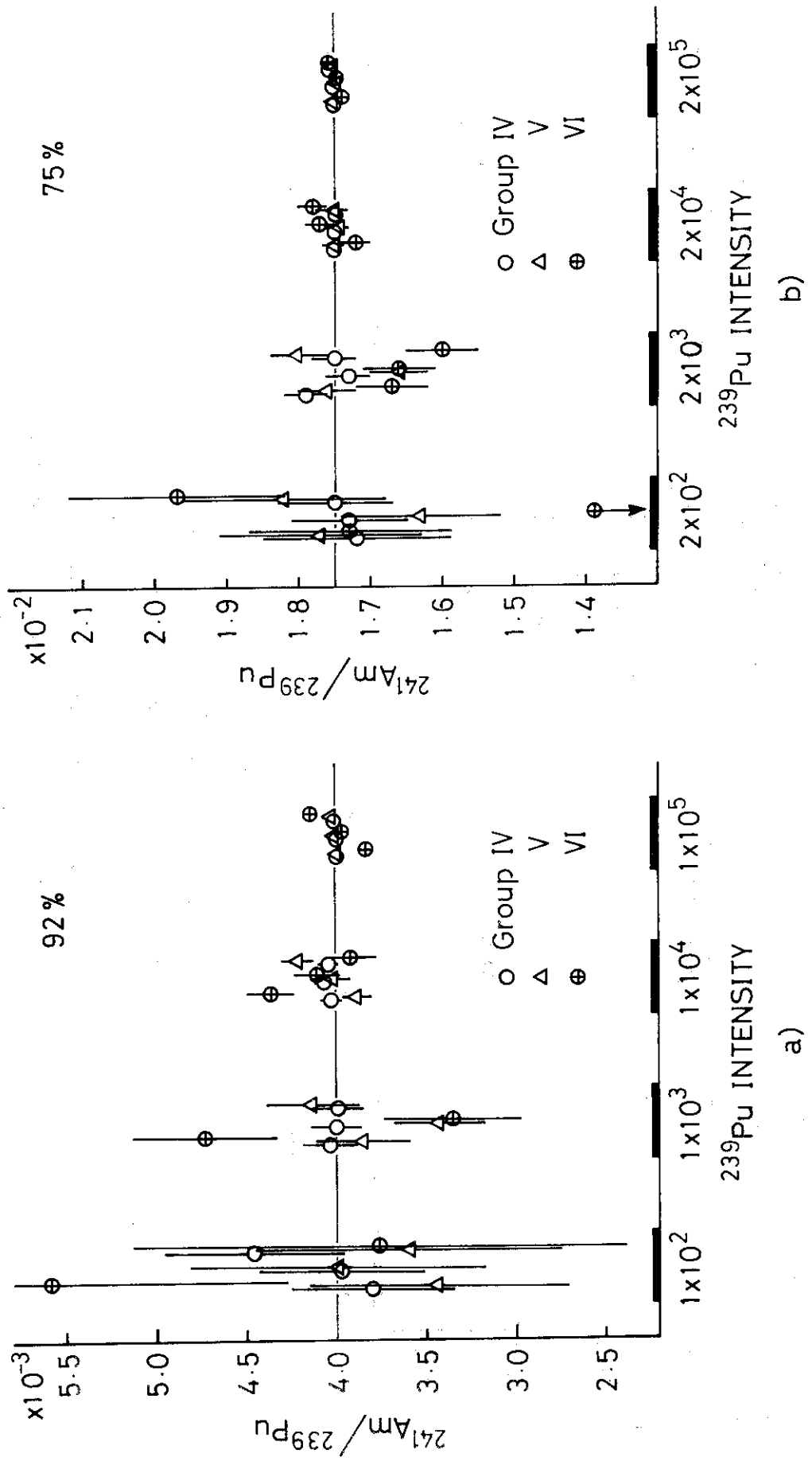

Fig.3. Relative abundance of ^{241}Am to ^{239}Pu versus statistical condition. Three peak groupings, IV, V, and VI, were the subject of study. For further details, see the caption of Fig.2.

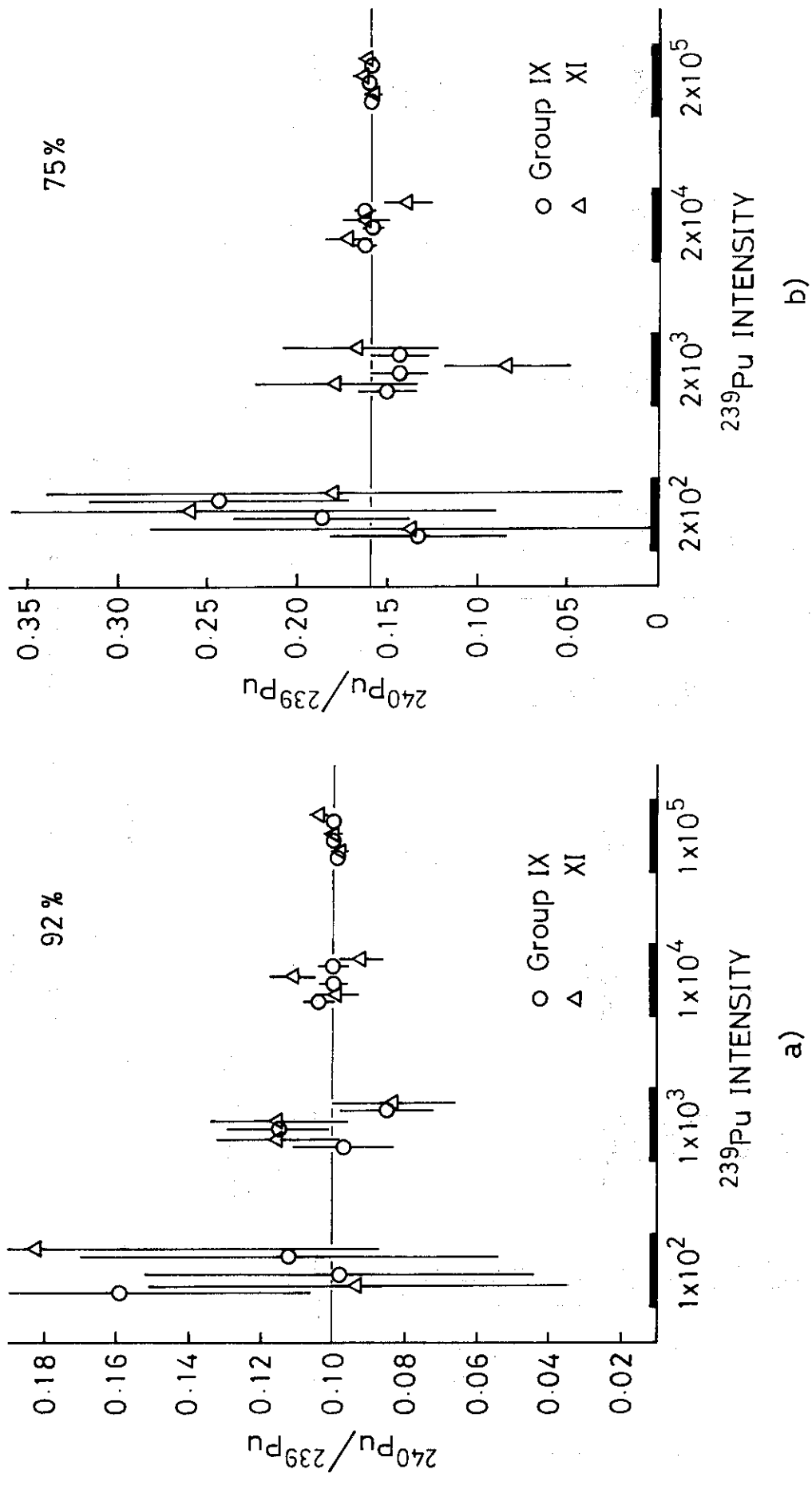

Fig.4. Relative abundance of ^{240}Pu to ^{239}Pu versus statistical condition. Two peak groupings, IX and XI, were the subject of study. For further details, see the caption of Fig.2.

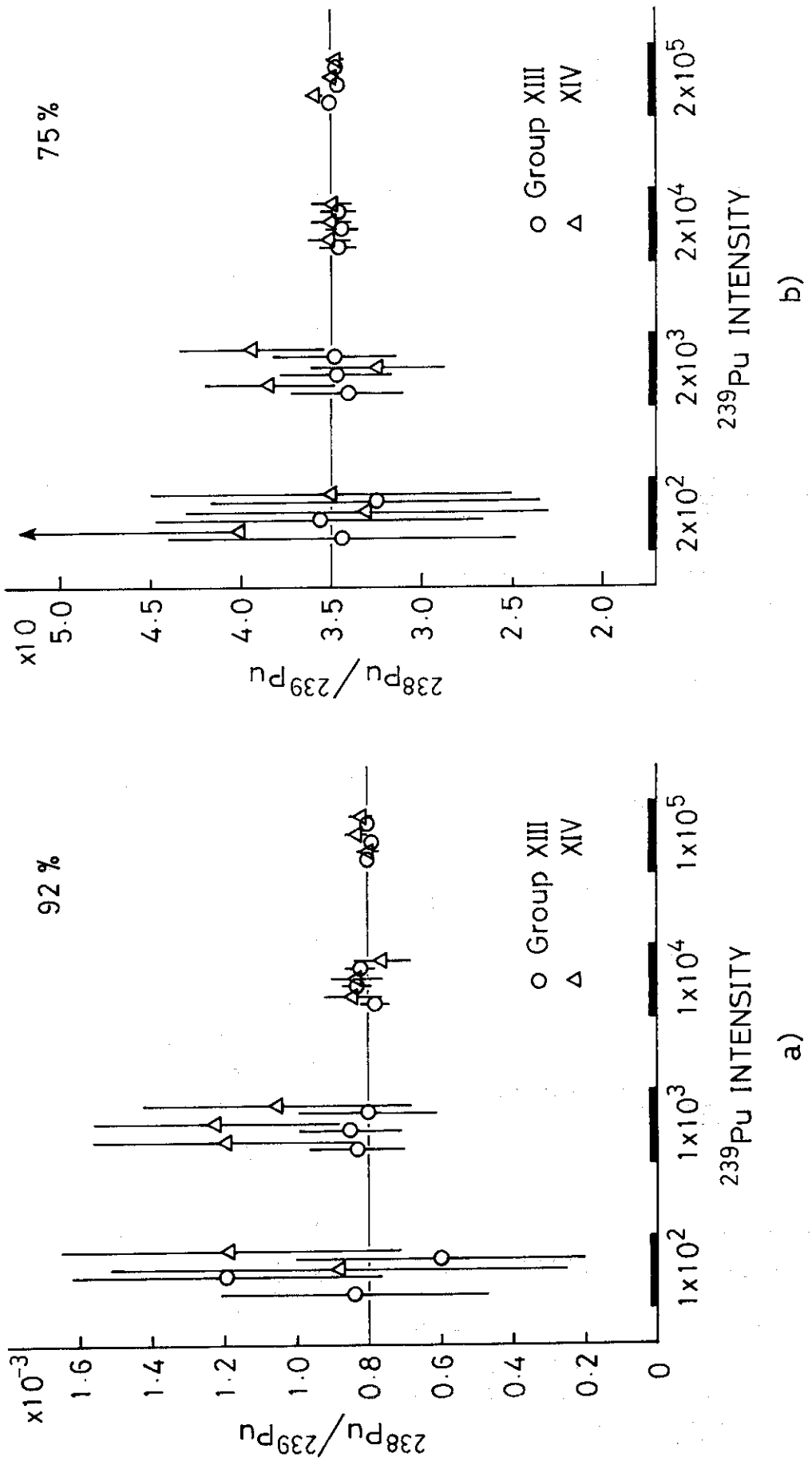

Fig.5. Relative abundance of ^{238}Pu to ^{239}Pu versus statistical condition. Two peak groupings, XIII and XIV, were the subject of study. For further details, see the caption of Fig.2.

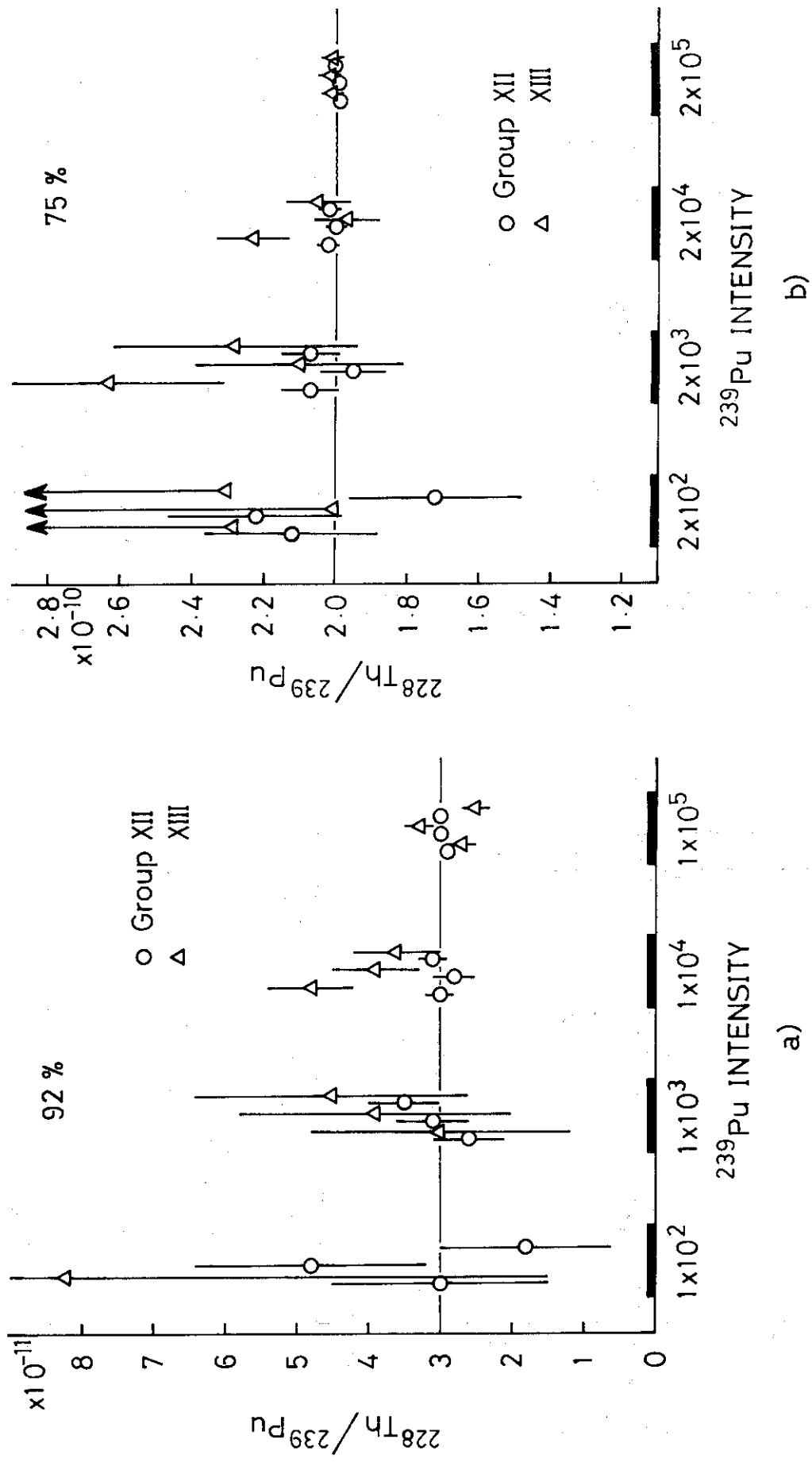

Fig.6. Relative abundance of ^{228}Th to ^{239}Pu versus statistical condition. Two peak groupings, XII and XIII, were the subject of study. For further details, see the caption of Fig.2.

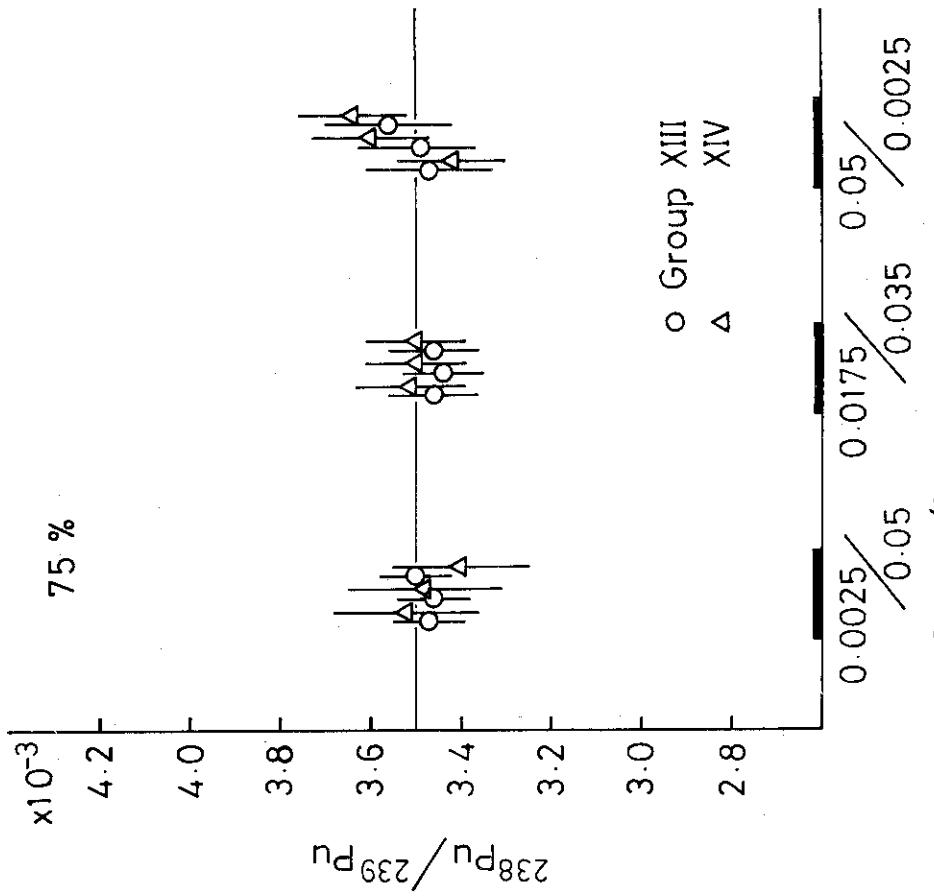

Fig.8. Aging effect on the precision of the relative abundance of ^{238}Pu for the case of the 75% ^{239}Pu sample. The variable of the abscissa is the ratio between $^{241}Am/^{239}Pu$ and $^{241}Pu/^{239}Pu$.

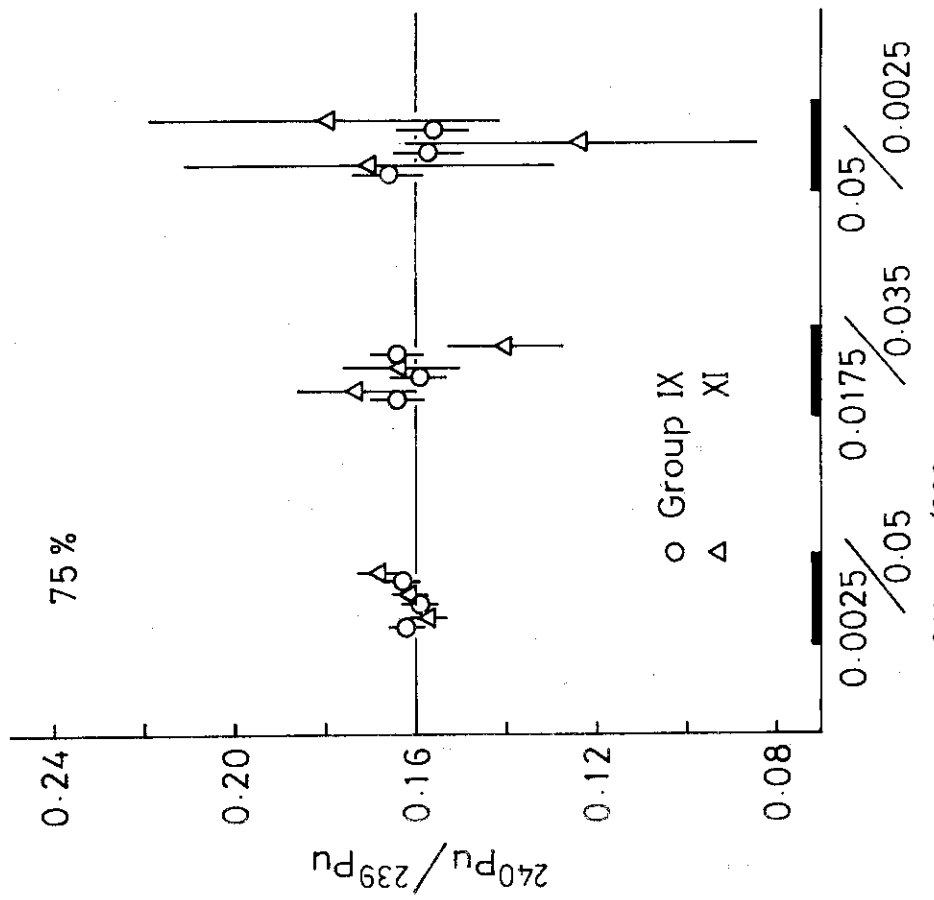

Fig.7. Aging effect on the precision of the relative abundance of ^{240}Pu for the case of the 75% ^{239}Pu sample. The variable of the abscissa is the ratio between $^{241}Am/^{239}Pu$ and $^{241}Pu/^{239}Pu$.

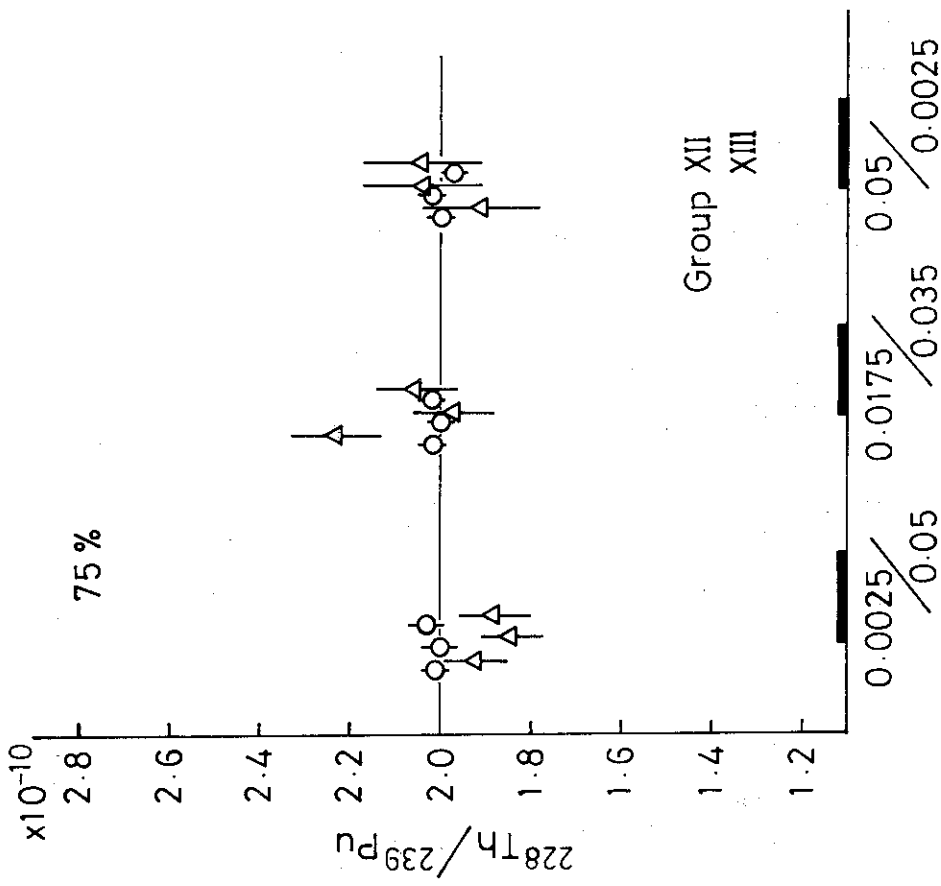

Fig.9. Aging effect on the precision of the relative abundance of ^{228}Th for the case of the 75% ^{239}Pu sample. The variable of the abscissa is the ratio between $^{241}Am/^{239}Pu$ and $^{241}Pu/^{239}Pu$.

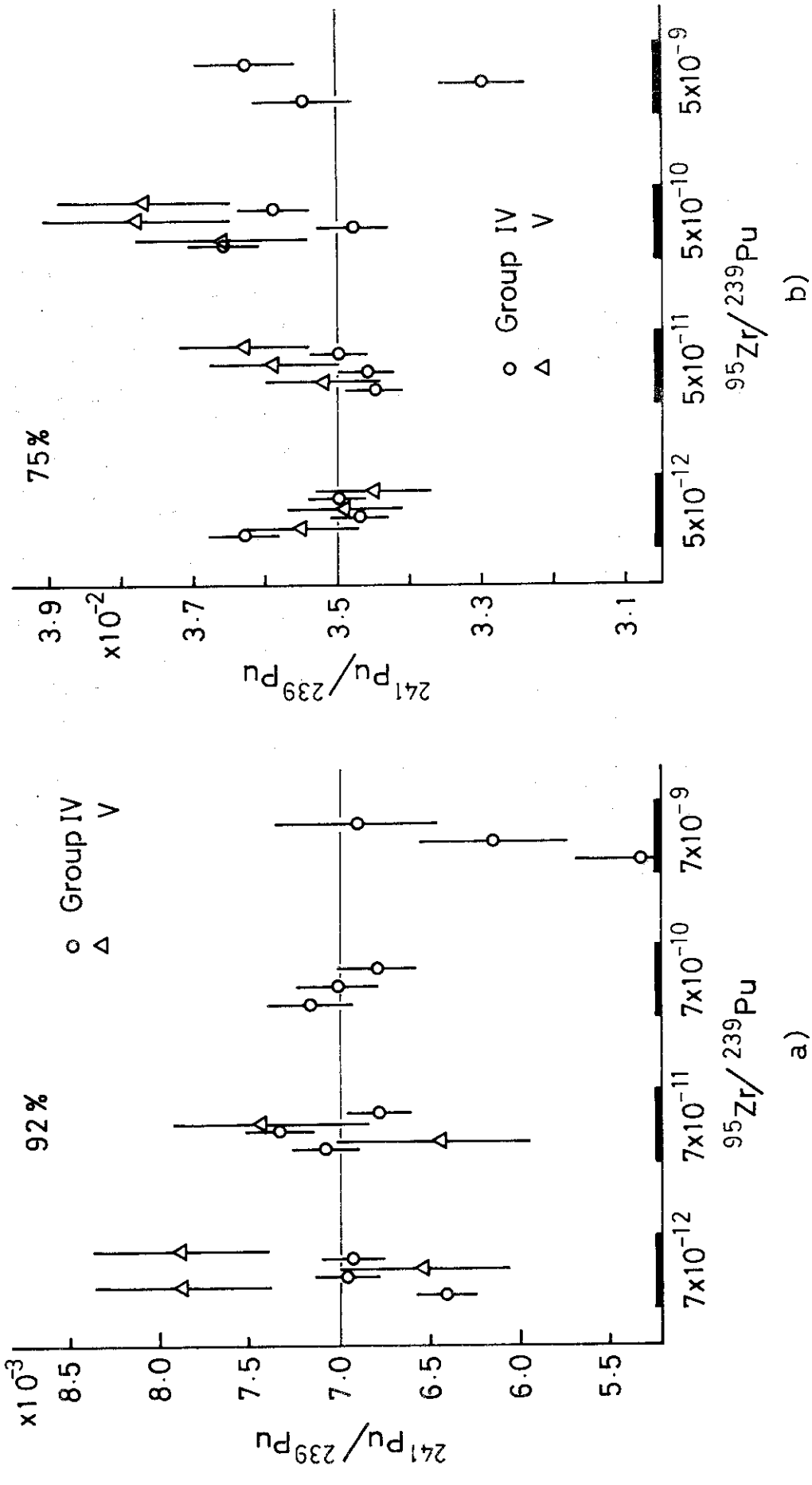

Fig.10. Effect of the FP contamination on the precision of the relative abundance of ^{241}Pu. The variable of the abscissa is the relative abundance of ^{95}Zr to ^{239}Pu.

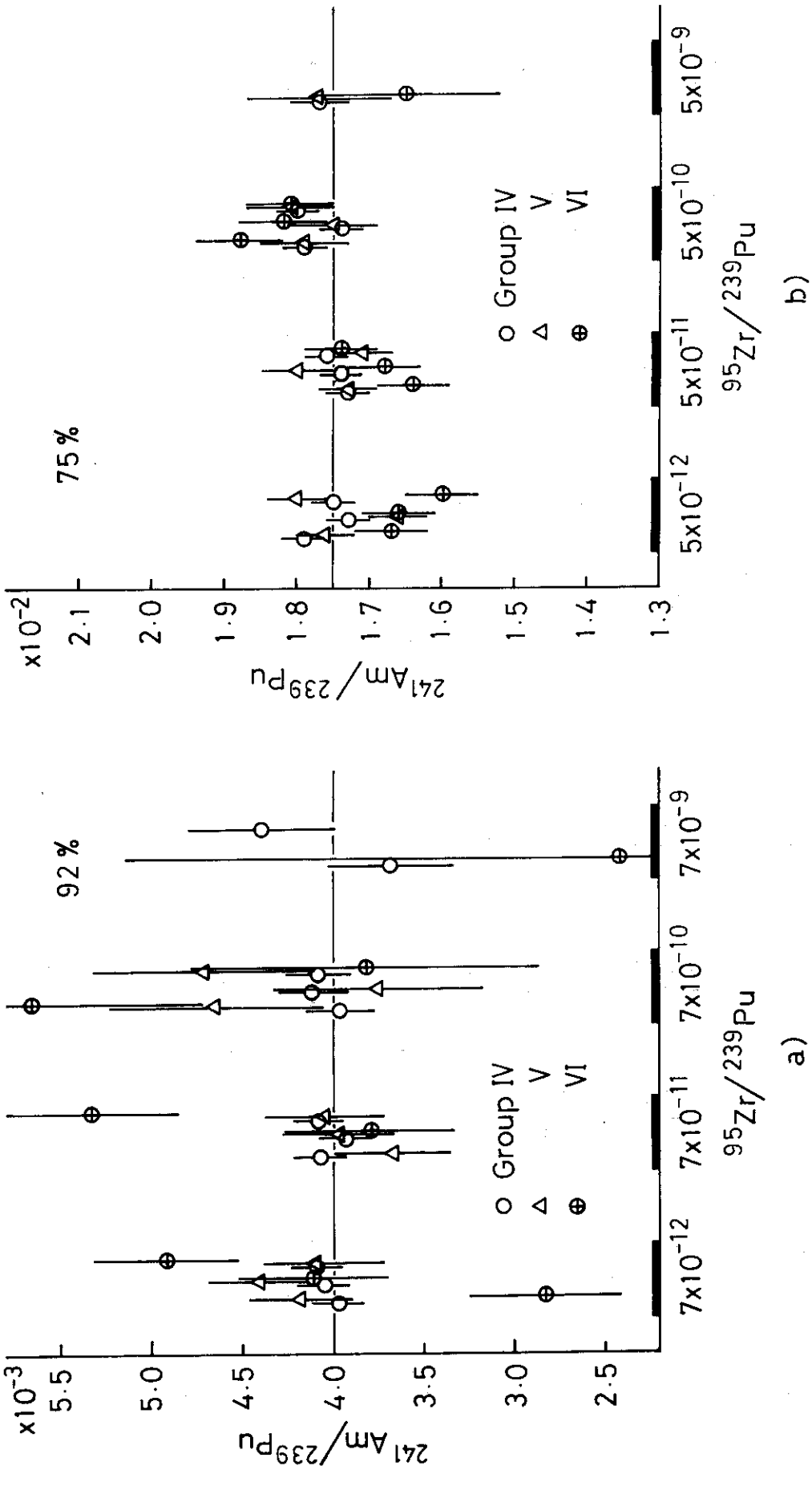

Fig.11. Effect of the FP contamination on the precision of the relative abundance of ^{241}Am. The variable of the abscissa is the relative abundance of ^{95}Zr to ^{239}Pu.

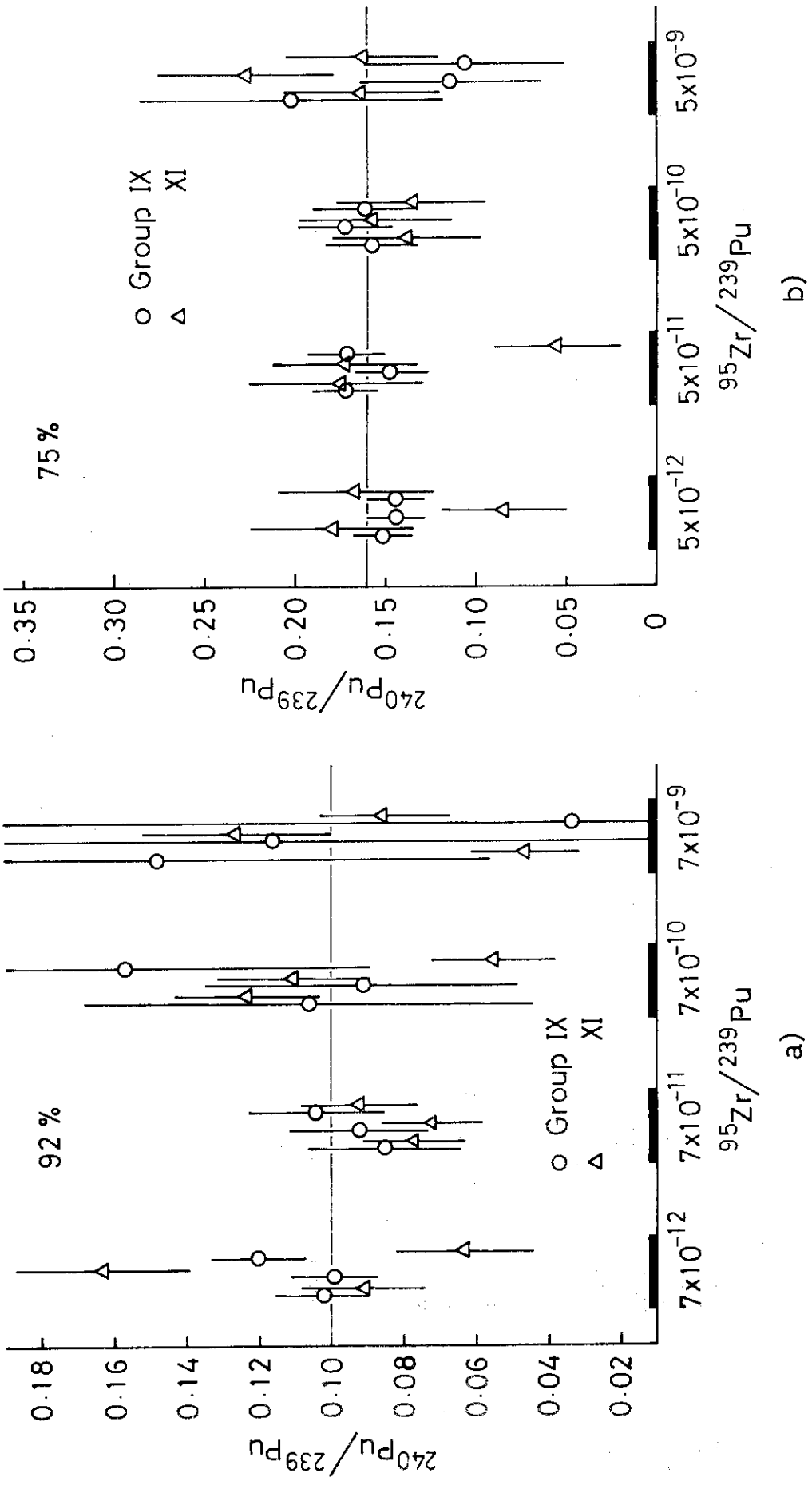

Fig.12. Effect of the FP contamination on the precision of the relative abundance of ^{240}Pu. The variable of the abscissa is the relative abundance of ^{95}Zr to ^{239}Pu.

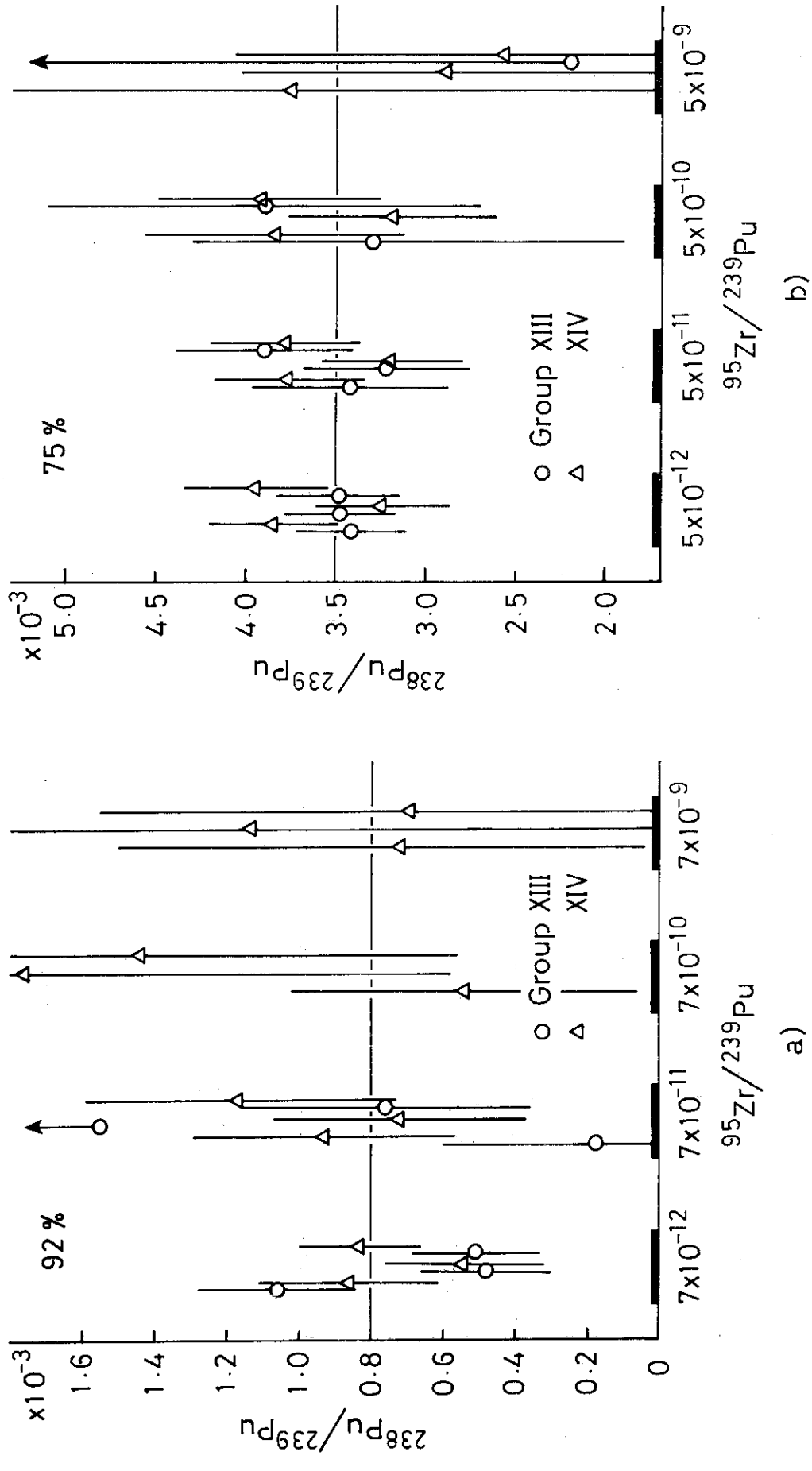

Fig.13. Effect of the FP contamination on the precision of the relative abundance of ^{238}Pu. The variable of the abscissa is the relative abundance of ^{95}Zr to ^{239}Pu.

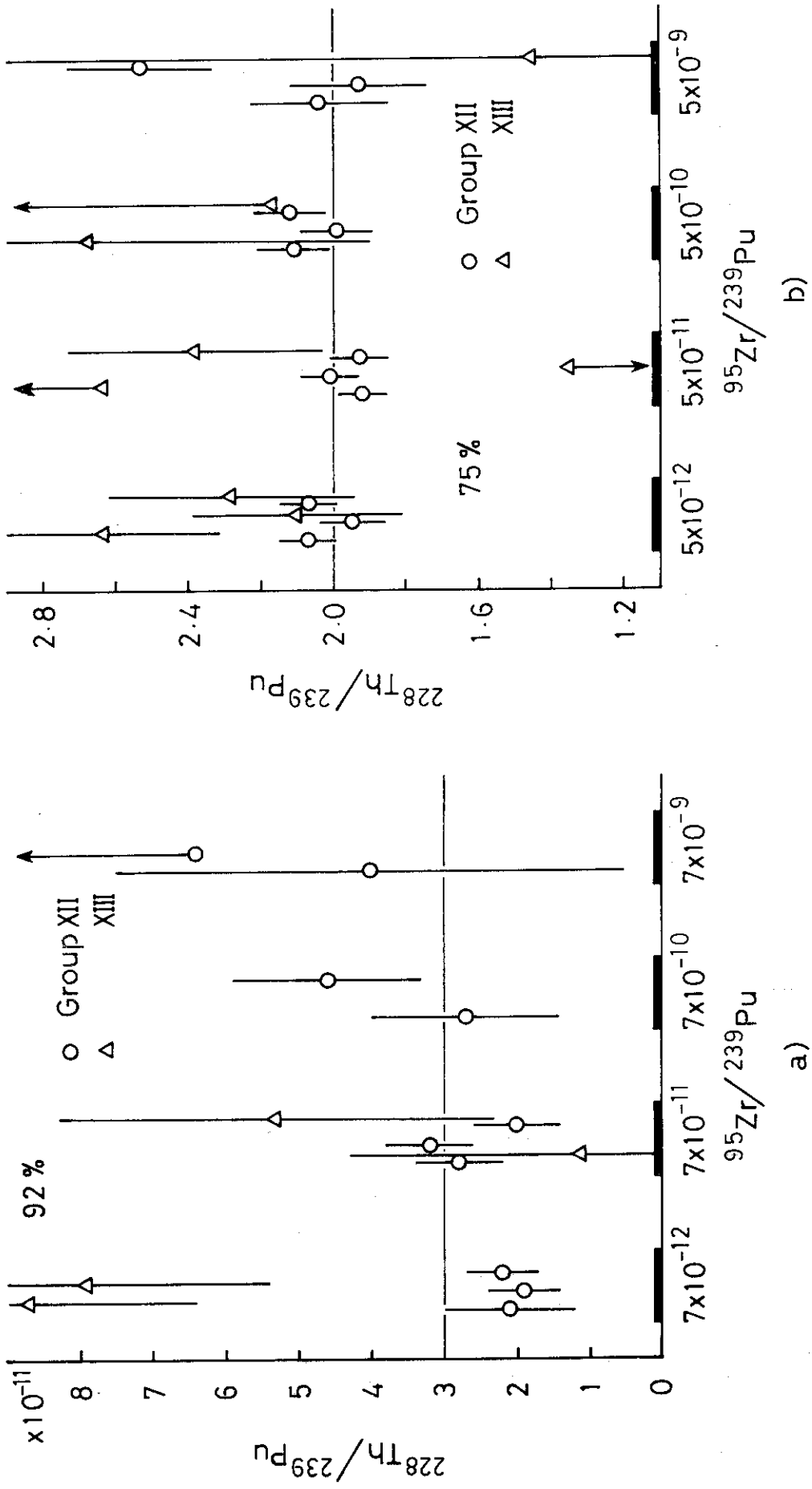

Fig.14. Effect of the FP contamination on the precision of the relative abundance of ^{228}Th. The variable of the abscissa is the relative abundance of ^{95}Zr to ^{239}Pu.